

An atomic colour superfluid via three-body loss

A. Kantian,¹ M. Dalmonte,^{1,2} S. Diehl,¹ W. Hofstetter,³ P. Zoller,¹ and A. J. Daley¹

¹*Institute for Theoretical Physics, University of Innsbruck, A-6020 Innsbruck, Austria*

and Institute for Quantum Optics and Quantum Information of the Austrian Academy of Sciences, A-6020 Innsbruck, Austria

²*Dipartimento di Fisica dell'Universit di Bologna and INFN, via Irnerio 46, 40127 Bologna, Italy*

³*Institute for Theoretical Physics, Johann Wolfgang Goethe-Universität, Frankfurt, Germany*

(Dated: June 15, 2018)

Large three-body losses in a three-component Fermi gas confined in an optical lattice can prevent the occupation of a lattice site by three atoms. This effective constraint not only gives rise to a suppression of actual three-body loss, but stabilises BCS pairing phases by suppressing the formation of trions. We study the effects of the constraint using bosonisation and density matrix renormalisation group techniques (DMRG). We discuss the case of lithium experiments, and study the dissipative dynamics including loss using time-dependent DMRG with quantum trajectories methods.

Recent developments in the experimental control of degenerate Fermi gases with cold atoms [1] has paved the way for the study of three-component Fermi mixtures [2]. For attractive two-body interactions, these systems offer a chance to observe competition between an atomic colour superfluid phase with BCS pairing and a trionic phase (with three particles on the same site) [3, 4, 5, 6]. A key feature of current experiments, though (e.g., with lithium), is the large three-body loss rate observed in these mixtures. Here we discuss how these losses, which are normally undesirable, can give rise to an effective three-body hard-core constraint [7, 8] when the gas is loaded into an optical lattice [9]. Not only does this suppress actual loss events, but it also acts to suppress trion formation, thus stabilising pairing phases such as the atomic colour superfluid. The blockade mechanism is related to the continuous quantum Zeno effect, and has been demonstrated for two-body interactions in an experiment with Feshbach molecules [10, 11]. The constraint has particularly striking consequences in 1D, where in the absence of such a constraint there is no atomic colour superfluid (ACS) phase, but rather competition between a charge-density wave (CDW) and a phase with symmetric (on-site) trions (ST) [4] (see Fig. 1a). We show that a constraint prevents ST formation and produces an ACS phase, which competes with a CDW and off-site trions (OT) (see Fig. 1b).

A three component Fermi gas in the lowest band of an optical lattice is described by the Hamiltonian ($\hbar = 1$)

$$H_U = - \sum_{\langle i,j \rangle, \sigma} J_\sigma (c_{i,\sigma}^\dagger c_{j,\sigma} + h.c.) + \sum_{i,\sigma} U_\sigma m_{i,\sigma} m_{i,\sigma+1}, \quad (1)$$

where $\langle i,j \rangle$ denotes a sum over neighbouring sites, $c_{i,\sigma}^\dagger, c_{i,\sigma}$ are fermionic operators with a species index $\sigma = 1, 2, 3$, $m_{i,\sigma} = c_{i,\sigma}^\dagger c_{i,\sigma}$, J_σ are the tunnelling amplitudes, and U_σ are the onsite interaction energy shifts. In the following, we will consider balanced densities $\bar{m}_\sigma = \bar{n}/3$ for total mean number density \bar{n} , and in typical realisations we will have equal tunnelling amplitudes $J_\sigma = J$. This model is valid in the limit $J_\sigma, U_\sigma \bar{n} \ll \omega$, with ω the

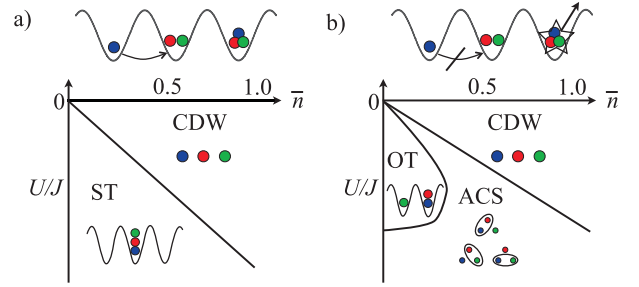


FIG. 1: Qualitative phase diagram for attractive interactions $U < 0$ and equal populations $\bar{n}/3$ of each component in a three-component 1D Fermi gas. These are shown in the SU(3) symmetric case (where all pairwise interactions between different components are of equal strength), a) without and b) with a three-body hard-core constraint arising from three-body loss. The unconstrained case is characterised by competition between symmetric (on-site) trions (ST) and a charge-density wave (CDW). The hard-core constraint suppresses trion formation, stabilising BCS pairing in an atomic colour superfluid (ACS), which competes with a CDW and off-site trions (OT).

energy separation between the lowest two Bloch bands.

Three-body recombination will result in decay into the continuum of unbound states, i.e., loss from the optical lattice. The decay dynamics can be described by a master equation in which loss occurs from a single site occupied by three atoms at a rate γ_3 [7],

$$\dot{\rho}^{(n)} = -i \left(H_{\text{eff}} \rho^{(n)} - \rho^{(n)} H_{\text{eff}}^\dagger \right) + \gamma_3 \sum_i t_i \rho^{(n+3)} t_i^\dagger,$$

where $\rho^{(n)}$ is the system density operator with n atoms, $t_i = c_{i,1} c_{i,2} c_{i,3}$, and the effective Hamiltonian is $H_{\text{eff}} = H_U - i\gamma_3 t_i^\dagger t_i / 2$. If we begin with an initial state not involving three body occupation, then via a mechanism analogous to the quantum Zeno effect, a large loss rate $\gamma_3 \gg J$ will suppress coherent tunnelling that would produce triply occupied sites. For large γ_3/J , loss occurs at an effective rate that decreases as J^2/γ_3 in second-order perturbation theory. Then, on a timescale where loss

can be neglected, the system dynamics is described by the constrained Hamiltonian

$$H_C = \mathcal{P}H_U\mathcal{P}, \quad \mathcal{P} = \prod_j \mathcal{P}_j = \prod_j (1 - m_{j,1}m_{j,2}m_{j,3}),$$

where \mathcal{P} is a projector onto the subspace of states with at most two atoms per site. We will initially consider the physics of this model, then return to the master equation in order to test the assumption that loss is small, and to investigate time-dependent preparation of states.

Below we focus on the case of a 1D gas, which allows us to make quantitative predictions for realistic experimental parameters using time-dependent density matrix renormalisation group (DMRG) methods [12] to compute both ground states and near-equilibrium time-evolution. The 1D case differs from higher dimensions due to the absence of spontaneous symmetry breaking, but provides a striking example of the effect of the hard-core constraint in that an ACS phase appears that is not present in the absence of the constraint. We first determine a qualitative phase diagram for the constrained model in the weakly interacting regime using Tomonaga Luttinger Liquid (TLL) bosonisation techniques, and then go beyond this limit by using time-dependent DMRG methods to compute the ground state within the constrained Hamiltonian. We treat both the SU(3) symmetric case where all interaction constants are equal (as could be realised, e.g., with alkaline earth atoms [13]), and the case where interactions are unequal (as are typical in Lithium experiments at low magnetic fields [2]). At the end we combine time-dependent DMRG techniques with quantum trajectory methods to investigate the production of an ACS state by computing time evolution for typical experimental parameters under the full master equation.

Bosonisation formalism for the constrained Hamiltonian:- In order to produce a qualitative phase diagram, we would like to apply the bosonisation formalism to our system. It is therefore necessary to implement the constraint in a more explicit way. We have identified an exact mapping of the constrained fermionic Hamiltonian H_C to an unconstrained fermionic Hamiltonian which automatically respects the constraint, at the expense of including higher order interactions. We introduce projected operators $d_{i\sigma}^\dagger = (\prod_{j \neq i} \mathcal{P}_j)c_{i\sigma}^\dagger$, $d_{i\sigma} = (\prod_{j \neq i} \mathcal{P}_j)c_{i\sigma}$, entirely in terms of which we express the Hamiltonian. We verify (i) that the operators $d_{i\sigma}$ obey fermionic commutations on the subspace where at most two atoms occupy any site, and that (ii) the Hamiltonian has vanishing matrix elements in the space with occupations greater than two and (iii) acts as zero on any state in this latter space. Thus, we arrive at a fermionic Hamiltonian with built-in constraint, which we analyse with standard bosonisation techniques. Here we summarise the results, with the calculations presented in more detail in a forthcoming work [14]. We introduce three bosonic fields $\phi_\sigma(x)$ related to the

continuum version of $(d_{i\sigma}^\dagger, d_{i\sigma})$, from which we can construct a Hamiltonian by taking the linear combinations $\phi_c = (\phi_1 + \phi_2 + \phi_3)/\sqrt{3}$, which represents collective fluctuations of the total density, and $\phi_{s1} = (\phi_1 - \phi_2)/\sqrt{2}$ and $\phi_{s2} = (\phi_1 + \phi_2 - 2\phi_3)/\sqrt{6}$, which represent the spin sectors. If we define TLL parameters K_α and conjugate momentum fields Π_α corresponding to each field ϕ_α ($\alpha \in \{c, s1, s2\}$), we then obtain

$$H = \sum_{\alpha=c,s1,s2} \left\{ \frac{v}{2} [K_\alpha \Pi_\alpha^2 + \frac{1}{K_\alpha} (\partial_x \phi_\alpha)^2] \right\} + \\ - \frac{2g_{ss}}{a^2} \cos[\sqrt{2\pi}\phi_{s1}] \cos[\sqrt{6\pi}\phi_{s2}] - \frac{g_s}{a^2} \cos[\sqrt{8\pi}\phi_{s1}],$$

where $v = 2aJ \sin[\pi\bar{n}/3]$ is the Fermi velocity, a is the lattice spacing. The coefficients g_{ss} and g_s exhibit non-trivial dependence on U/J and \bar{m}_σ , as do K_α .

Correlation functions:- To identify the dominant correlations and determine a phase diagram, we consider the behaviour of correlation functions related to different ordering: CDW (for which we compute density-density correlations $C(x) \propto \langle n_i n_{i+x} \rangle$), ACS (with BCS correlations $P_\sigma(x) \propto \langle d_{i,\sigma}^\dagger d_{i,\sigma+1}^\dagger d_{i+x,\sigma} d_{i+x,\sigma+1} \rangle$) and OT ($OT(x) \propto \langle \tilde{t}_{i,\sigma}^\dagger \tilde{t}_{i+x,\sigma} \rangle$ with $\tilde{t}_{i,\sigma} = d_{i,\sigma} d_{i,\sigma+1} d_{i+1,\sigma+2}$). Each correlation is characterized by a scaling dimension that determines its algebraic decay. The decay exponents for CDW and ACS order are independent of σ in the SU(3) symmetric case and can be related to TLL parameters as: $\mathcal{D}_{CDW} = 2K_c/3 + K_{s1}/3 + K_{s2}$, $\mathcal{D}_{ACS} = K_{s1} + 2/(3K_c) + 1/(3K_{s2})$. Correlations for OT order have multiple contributions in terms of bosonic operators, with two distinct decay exponents in the SU(3) case, $\mathcal{D}_{OT}^I = 3/(2K_c) + 3K_c/2$ and $\mathcal{D}_{OT}^{II} = 3/(2K_c) + K_c/6 + 4K_{s2}/3$. We can then extract values of the decay exponents as a function of U/J and \bar{n} by expanding K_α in the weak interaction limit. These can be compared to determine a phase diagram, and also benchmarked against values extracted from numerical simulations (see Table I).

Phase diagram from bosonisation (equal interactions):- The 1D model H_U without the hard-core constraint has been previously studied for attractive interactions using a combination of the TLL formalism and DMRG methods [4]. The qualitative phase diagram is depicted in Fig. 1a, and involves competition between symmetric (on-site) trion (ST) order and charge-density-wave (CDW) order. In a wide region near the SU(3) symmetric line $U_\sigma = U < 0$, CDW is dominant for higher densities and intermediate interactions. A particular feature of this system with $U < 0$ is that a gap appears in the entire spin sector, so that in contrast to a two-species Fermi gas, ACS correlations decay exponentially (as do spin-density wave correlations).

In the presence of the constraint this picture changes substantially (see Fig. 1b with small $|U/J|$). Outside a small region at low densities $\bar{n} < 0.2$ and intermediate interactions, where off-site trionic correlations compete

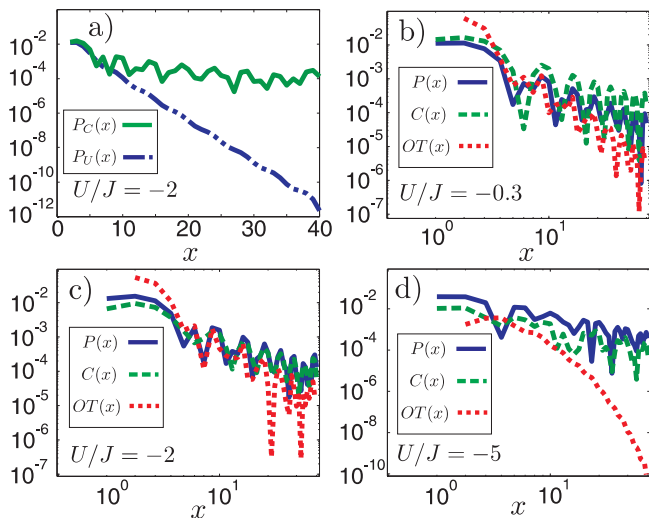


FIG. 2: a) ACS-correlations $P_\sigma(x)$ with (solid line) and without (dash-dotted line) the three-body constraint as a function of distance x on a 40 site lattice. b) - d) $P_\sigma(x)$ with CDW-correlations $C(x)$ and off-site trion correlations $OT(x)$ for different values of U , at a density $\bar{m}_1 = \bar{m}_2 = \bar{m}_3 = 0.2$, with the constraint. In qualitative agreement with bosonisation, we observe that (b) for weak coupling CDW clearly dominates. As the coupling increases (c, d), ACS becomes stronger relative to CDW. For the values presented here, ACS dominates off-site trions, with $OT(x)$ decaying exponentially for strong coupling.

with CDW, the spin sector is gapless and all correlation functions decay algebraically. The ST phase is suppressed by the constraint, and is replaced by a competition between off-site trions (OT), and an ACS phase with simultaneous pairing of all three pairs of components.

Phase diagram from bosonisation (unequal interactions):- In the case of unequal interactions, the spin and charge sectors are coupled by additional terms $H_{cross} = \lambda_{cs2} \partial_x \phi_c \partial_x \phi_s^2 + \lambda_{cs1} \partial_x \phi_c \partial_x \phi_{s1} + \lambda_{ss} \partial_x \phi_{s1} \partial_x \phi_{s2}$, with $\lambda_{cs2} = \sqrt{2}(2U_1 - U_2 - U_3)/(6\pi v)$, and $\lambda_{cs1}/\sqrt{6} = (U_3 - U_2)/(6\pi v) = -\lambda_{ss}/\sqrt{3}$. When the interaction imbalance is strong enough to couple different sectors, opening of a gap in the spin sector can enhance one-channel pairing with respect to the other, and we obtain pairing between the species with the strongest attractive interaction.

Ground state computations with time-dependent DMRG (equal interactions) :- In order to quantitatively underpin these results and to go beyond the weak-coupling regime, we present calculations based on time-dependent DMRG methods [12]. In Fig. 2a, we see again the striking comparison between the ACS correlations in the ground states for H_U and H_C , which exhibit exponential decay without the hard-core constraint, and algebraic decay in the presence of the constraint. In Figs. 2b-c we show a comparison of the correlations corresponding to the ACS ($P_\sigma(x)$), CDW

$-U/J$	\mathcal{D}_{ACS}	\mathcal{D}_{CDW}	\mathcal{D}_{OT}
0.3	1.71(0.02)/2.04	1.39(0.02)/1.95	3.3(0.3)/3.00
0.6	1.66(0.02)/2.03	1.40(0.03)/1.96	3.3(0.3)/3.00
1	1.60(0.02)	1.40(0.03)	3.1(0.4)
2	1.4(0.2)	1.4(0.1)	3.0(0.4)
5,8,10	1.4(0.4)	1.4(0.3)	exp

TABLE I: Exponents for algebraic decay of correlations, computed for ground states in a system of 40 lattice sites with $\bar{m}_\sigma = 0.2$ by fitting a power law to the periodic peaks of the correlations (see Fig. 2). Errors are given in parentheses, analytic values in the weak coupling limit are given to the right of slashes. We find agreement with the qualitative predictions of analytic theory, i.e. for weak coupling we start out with the CDW-phase dominant, from where \mathcal{D}_{CDW} remains constant whilst \mathcal{D}_{ACS} and \mathcal{D}_{OT} decrease with increasing $|U/J|$. We further observe a transition to exponential decay for the off-site trions in the strong coupling limit.

($C_\sigma(x)$) and OT ($OT(x)$), in the ground state of the model with a three-body hard-core constraint (H_C). These are presented for symmetric but varying interactions from weak to strong coupling, $U/J \in [-10, -0.3]$. For increasing interactions, the values of $P_\sigma(x)$ become stronger compared with $C_\sigma(x)$, so that the ACS appears to dominate for stronger interactions. While off-site trions still show algebraic decay for $U/J \geq -2$, they are subdominant to the ACS and CDW, and they decay exponentially for $U/J \leq -5$ (Figs. 2 b-d). This is a strong deviation from the weak-coupling bosonisation results, and could indicate an instability (e.g., towards phase separation), or the appearance of a gap in the dual field of the charge sector. However, with system sizes of 40 lattice sites, we have not observed any evidence of phase separation.

Extracting the exponents of the algebraic decay of the correlation functions further confirms this picture, as shown in Table 1. The constrained model sees an enhancement of ACS correlations with decreasing U , while CDW correlations generally decay faster as U is lowered. In the weak coupling regime we also generally observe good agreement with the perturbative values of the exponents from TLL-theory. In the strong coupling regime ($U/J \leq -5$) for the constrained case, the exponents \mathcal{D}_{ACS} and \mathcal{D}_{CDW} saturate, with \mathcal{D}_{ACS} taking a value compatible with the TLL prediction $\mathcal{D}_{ACS}^{TLL} = 2/(3K_c) + 4/3$ in the case where $2/(3K_c) \rightarrow 0$. This is consistent with either an instability ($K_c \rightarrow \infty$), or Π_c becoming massive.

Ground state computations with time-dependent DMRG (unequal interactions):- In the case of asymmetric interactions we also observe an ACS pairing, but with only the two components paired that exhibit the strongest interactions. As an example, we consider the case of ${}^6\text{Li}$, where in Fig. 3a we plot the Hamiltonian parameters as a function of magnetic field strength near

500-700 G for a fixed lattice depth. From the pairing correlations shown in Fig. 3b, we see that at 520 G, the only algebraically decaying correlations are those corresponding to components 1 and 3, which have the strongest interparticle interaction.

Time-dependent preparation of states:- Considering this example, we now return to the full time-dependent dynamics including three-body loss, in order to demonstrate a method to produce these ACS states in ${}^6\text{Li}$. We simulate the many-body master equation on 12-24 lattice sites by combining time-dependent DMRG methods with quantum trajectories techniques, as described in [7]. We assume that the lattice is initially loaded at a magnetic field of 615 G, where the repulsive interactions (see Fig. 3a) will stabilise the system in the presence of loss. We then consider a time-dependent ramp of the magnetic field to 500 G. The characteristics of the ramp we choose (shown in Fig. 3c) are: (i) it is adiabatic until 565 G, where the components 2 and 3 become paired, (ii) it is fast from 565 – 500 G, where onsite trions become energetically favoured ($\sum_{\alpha} U_{\alpha} < U_2$) and where for fields larger than 520 G, γ_3 is too small to prevent triple occupation (see Fig. 3a), and (iii) after a hold time $T_{h,1} = 16J^{-1}$ we add a swap between species 1 and 2 via a fast laser pulse at the end of the ramp, after which there is a second hold time $T_{h,2} = 20J^{-1}$. The ACS correlations in the final state after the swap (Fig. 3d) then exhibit dominant pairing between species 1 and 3, as would be expected in the ground state for the parameters of ${}^6\text{Li}$ at $B = 500$ G with the constraint. At the same time, the other two pairing channels are clearly subdominant as evidenced by their much weaker correlators, while trion formation is also strongly suppressed during the ramp. Further, the probability that not even a single decay event occurs during the ramp shown here is $\sim 80\%$ for 12 lattice sites.

These ideas can be extended to higher dimensions, where the ACS should also be stabilised due to suppressed trion formation.

We thank S. Jochim, M. Fleischhauer, P. Julienne, M. Baranov, and E. Ercolessi for discussions. This work was supported by the Austrian Science Foundation (FWF) through SFB F40 FOQUS and project I118_N16 (EuroQUAM_DQS), the DARPA OLE program, and by the Austrian Ministry of Science BMWF via the UniInfrastrukturprogramm of the Forschungsplattform Scientific Computing and Centre for Quantum Physics Innsbruck. WH acknowledges support by the DFG through SFB/TR 49.

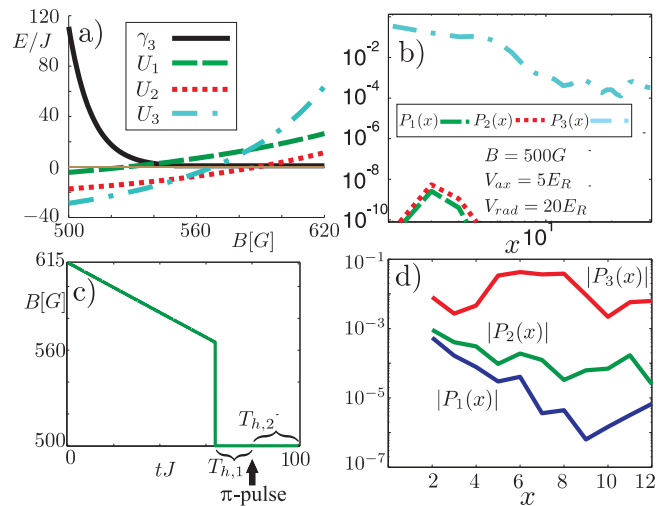


FIG. 3: a) Hubbard parameters U_1 , U_2 , U_3 and three-body loss rate γ_3 for ${}^6\text{Li}$ as function of external magnetic field B , for a lattice depth of $V_{ax} = 5 E_R$ in axial direction, and $V_{rad} = 20 E_R$ in radial direction. b) ACS correlations for the ground state of H_C at $B = 500$ G, computed for a system of 30 lattice sites, $\bar{m}_\sigma = 2/15$, $\sigma = 1, 2, 3$. The solid line shows $P_3(x)$, dashed line $P_1(x)$, dotted line denotes $P_2(x)$. As $U_3 < U_2 \ll U_1$, we see 1 – 3 pairing dominate, with all other pairing exponentially suppressed. c) Magnetic field $B(t)$ for the adiabatic ramp. d) ACS correlations after the time-dependent ramp of the magnetic field shown in (c), beginning from the ground state at 615 G, with $\bar{m}_\sigma = 0.16$, on 12 sites.

[1] R. Jördens *et al.*, Nature (London) **455**, 204 (2008); C. H. Schunck, Y. Shin, A. Schirotzek, and W. Ketterle, *ibid.* **454**, 739 (2008); J. T. Stewart, J. P. Gaebler, and

D. S. Jin, *ibid.*, 744 (2008); U. Schneider *et al.*, Science **322**, 1520 (2008); E. Wille *et al.*, Phys. Rev. Lett. **100**, 053201 (2008); A. Schirotzek, C.-H. Wu, A. Sommer, and M. W. Zwierlein, *ibid.* **102**, 230402 (2009).
 [2] T. B. Ottenstein *et al.*, Phys. Rev. Lett. **101**, 203202 (2008).
 [3] A. Rapp, G. Zarand, C. Honerkamp, and W. Hofstetter, Phys. Rev. Lett **98**, 160405 (2007); A. Rapp, W. Hofstetter and G. Zarand, Phys. Rev. B **77**, 144520 (2008).
 [4] S. Capponi *et al.*, Phys. Rev. A **77**, 013624 (2008); S. Capponi *et al.*, arXiv:0811.0555v1.
 [5] A. Modawi and A. Leggett, J. Low Temp. Phys. **109**, 625 (1997).
 [6] R. W. Cherng, G. Refael, and E. Demler, Phys. Rev. Lett. **99**, 130406 (2007).
 [7] A. J. Daley *et al.*, Phys. Rev. Lett. **102**, 040402 (2009).
 [8] M. Roncaglia, M. Rizzi, and J. I. Cirac, arXiv:0905.1247.
 [9] I. Bloch, J. Dalibard, and W. Zwerger, Rev. Mod. Phys. **80**, 885 (2008).
 [10] N. Syassen *et al.*, Science **320**, 1329 (2008).
 [11] J. J. Garcia-Ripoll *et al.*, arXiv:0809.3679v1.
 [12] G. Vidal, Phys. Rev. Lett. **93**, 040502 (2004); F. Verstraete, V. Murg, and J. I. Cirac, Adv. Phys. **57**, 143 (2008); A. J. Daley *et al.*, J. Stat. Mech.: Theor. Exp. P04005 (2004); S.R. White and A.E. Feiguin, Phys. Rev. Lett. **93**, 076401 (2004); F. Verstraete, J. J. Garcia-Ripoll, and J. I. Cirac, *ibid.* **93**, 207204 (2004).
 [13] A. V. Gorshkov *et al.*, arXiv:0905.2610.
 [14] M. Dalmonte *et al.*, in preparation.
 [15] A.O. Gogolin, A.A. Nersesyan, A.M. Tsvelik, *Bosoniza-*

tion and strongly correlated systems, (Cambridge University press, Cambridge, 1998); T. Giamarchi, *Quantum Physics in one dimension*, (Oxford University press, Ox-

ford, 2003).